Disease Activity in Mitral Annular Calcification - a Multimodality Study

Circulation: Cardiovascular Imaging

ORIGINAL ARTICLE

Disease Activity in Mitral Annular Calcification

A Multimodality Study

BACKGROUND: Mitral annular calcification (MAC) is associated with cardiovascular events and mitral valve dysfunction. However, the underlying pathophysiology remains incompletely understood. In this prospective longitudinal study, we used a multimodality approach including positron emission tomography, computed tomography, and echocardiography to investigate the pathophysiology of MAC and assess factors associated with disease activity and progression.

METHODS: A total of 104 patients (age 72±8 years, 30% women) with calcific aortic valve disease, therefore predisposed to MAC, underwent ^{18}F-sodium fluoride (calcification activity) and ^{18}F-Fluorodeoxyglucose (inflammation activity) positron emission tomography, computed tomography calcium scoring, and echocardiography. Sixty patients underwent repeat computed tomography and echocardiography after 2 years.

RESULTS: MAC (mitral annular calcium score >0) was present in 35 (33.7%) patients who had increased ^{18}F-fluoride (tissue-to-background ratio, 2.32 [95% CI, 1.81–3.27] versus 1.30 [1.22–1.49]; P<0.001) and ^{18}F-Fluorodeoxyglucose activity (tissue-to-background ratio, 1.44 [1.37–1.58] versus 1.17 [1.12–1.24]; P<0.001) compared with patients without MAC. MAC activity (^{18}F-fluoride uptake) was closely associated with the local calcium score and ^{18}F-Fluorodeoxyglucose uptake, as well as female sex and renal function. Similarly, MAC progression was closely associated with local factors, in particular, baseline MAC. Traditional cardiovascular risk factors and calcification activity in bone or remote atherosclerotic areas were not associated with disease activity nor progression.

CONCLUSIONS: MAC is characterized by increased local calcification activity and inflammation. Baseline MAC burden was associated with disease activity and the rate of subsequent progression. This suggests a self-perpetuating cycle of calcification and inflammation that may be the target of future therapeutic interventions.

Daniele Massera, MD, MSc
Maria G. Trivieri, MD, PhD
Jack P.M. Andrews, MD
Samantha Sartori, PhD
Ronan Abgral, MD, PhD
Andrew R. Chapman, MD
William S.A. Jenkins, MD
Alex T. Vesey, MD
Mhairi K. Doris, MD
Tania A. Pawade, MD, PhD
Kang H. Zheng, MD
Jorge R. Kizer, MD, MSc
David E. Newby, MD, PhD
Marc R. Dweck, MD, PhD

Drs Massera and Trivieri are joint first authors.

Key Words: disease progression ■ inflammation ■ mitral valve ■ positron emission tomography computed tomography

https://www.ahajournals.org/journal/circimaging

CLINICAL PERSPECTIVE

Mitral annular calcification (MAC) is associated with cardiovascular events and mitral valve dysfunction, but its pathophysiology is incompletely understood. We employed a multimodality imaging approach including ^{18}F-fluorodeoxyglucose and ^{18}F-sodium fluoride positron emission tomography, computed tomography calcium scoring, and echocardiography to investigate the pathology of MAC and elucidate the factors associated with its prevalence, disease activity, and disease progression. Patients who had MAC (34% of patients) had increased inflammatory and calcification activity by positron emission tomography imaging in the mitral annulus. Furthermore, calcification activity was most closely associated with computed tomography-MAC calcium score, inflammation, female sex, and renal dysfunction. Similarly, MAC progression on repeat computed tomography scans after 2 years was closely associated with baseline MAC, with the fastest rate of progression found in those with high baseline computed tomography-MAC scores and the highest calcification activity. By contrast, traditional cardiovascular risk factors and calcification activity in bone or remote atherosclerotic areas were not associated with disease activity nor progression. This suggests that MAC activity and progression are characterized by a vicious cycle of established calcium, injury and inflammation within the valve that prompts further calcification activity. These findings support the concept that therapeutic strategies targeting MAC will need to focus on breaking this vicious calcification cycle.

Mitral annular calcification (MAC) is a common finding on cardiovascular imaging studies with an estimated prevalence ranging from 8% to 42% depending on age of the population studied and analysis method.[1,2] Often associated with aortic, coronary artery, and aortic valve calcification (AVC),[2] MAC has been linked to increased atherosclerotic burden,[2] incident stroke,[3] and cardiovascular mortality.[4] Although MAC is associated with endothelial damage, lipid infiltration, and progressive valve calcification,[5–7] the pathophysiology of MAC remains incompletely understood and medical therapies to halt its progression are lacking. MAC also has functional consequences, helping to drive progressive mitral stenosis and mitral regurgitation, the severe stages of which can only be remedied through surgical or, potentially, percutaneous intervention.[8,9]

Several epidemiological studies have investigated risk factors for MAC, finding similar determinants as for calcific aortic valve disease, including age, obesity, smoking, and serum phosphate.[10,11] Important differences have also been observed, with MAC showing female predominance[7] and a stronger association with chronic kidney disease and dysregulated mineral metabolism.[12,13] An association with low bone mineral density (BMD) has been suggested but remains unproven.[14] Despite the various investigations into risk factors for MAC incidence and prevalence, no studies to date have evaluated risk factors governing disease activity.

Hybrid positron emission and computed tomography (PET-CT) allows for the simultaneous noninvasive evaluation of disease activity and heart valve anatomy.[15,16] CT provides a detailed assessment of calcium burden, and PET can measure the activity of specific disease processes dependent on the availability of suitable tracers. ^{18}F-Sodium fluoride (^{18}F-fluoride) is a marker of vascular and valvular calcification activity[17] that has been used to investigate vascular atherosclerosis and aortic stenosis.[15,18] ^{18}F-Fluorodeoxyglucose (^{18}F-FDG) has been used to measure vascular inflammation because of its accumulation within tissue macrophages.[19]

In this clinical imaging study, our aim was to use a state-of-the-art multimodality imaging approach to investigate activity and inflammation to elucidate factors associated with disease prevalence, activity, and progression.

METHODS

Patients aged >50 years with calcific aortic valve disease were recruited as previously described and formed the study cohort.[15] All had AVC on CT and were, therefore, deemed prone to developing calcific valve disease. Exclusion criteria included insulin-dependent diabetes mellitus, blood glucose >200 mg/dL, end-stage renal disease, metastatic malignancy, and life expectancy <2 years. The study cohort was divided into patients who did (score>0) or did not (score=0) have MAC on CT to assess factors associated with MAC prevalence. Clinical data were ascertained based on detailed history and clinical examination. Fasting serum biomarkers were analyzed as previously described. Lipoprotein(a) was measured using chemiluminescent immunoassays as previously described.[20] A detailed echocardiographic exam was performed under standardized conditions according to a formal protocol as previously described.[15] The Institutional Review Board of the University of Edinburgh approved the protocol, and participants provided written informed consent. Study data can be made available to other researchers on request to the corresponding author.

A control cohort without evidence of heart valve calcification (CT calcium score of 0 in mitral annulus and aortic valve) was also included to determine the normal range of ^{18}F-fluoride PET uptake in the mitral annulus, with the highest ^{18}F-fluoride tissue-to-background ratio (TBR_{max}) values defining the upper limit of normal and differentiating between study cohort patients who did (PET+) and did not have (PET–) increased PET activity.

PET-CT Imaging

PET-CT scans of the heart and aorta were performed with a hybrid scanner (Biograph mCT, Siemens Medical Systems, Erlangen, Germany). Two scans were performed at least 24 hours apart, 60 minutes after administration of ^{18}F-fluoride 125 MBq and 90 minutes after ^{18}F-FDG 200 MBq. ECG-gating was not used, and all counts were used for analysis. All patients were asked to adhere to a carbohydrate-free diet for 24 hours preceding their ^{18}F-FDG scan to suppress myocardial uptake, as previously described.[15] Patients were given a list of foods (high in fat and low in carbohydrate) to eat and also those to avoid. An ECG-gated breath-hold CT scan (noncontrast-enhanced, 40 mA/rot [CareDose], 100 kV) of the heart was performed for calcium scoring.

Image Analysis: CT

Mitral annulus, aortic valve, coronary artery, and aortic CT calcium scores were determined using dedicated analysis software (VScore, Vital Images, Minnetonka, and OsiriX Lite version 8.5.1, OsiriX Imaging Software, Geneva, Switzerland). Agatston scores were calculated using a threshold of 130 Hounsfield units.[21] MAC on (CT-MAC) was defined as calcium score >0 Agatston units (AU) in the mitral annulus.

Image Analysis: PET

Mitral annular ^{18}F-fluoride and ^{18}F-FDG PET activity were quantified according to a standardized protocol using OsiriX. Regions of interest were drawn around maximal areas of ^{18}F-fluoride and ^{18}F-FDG activity to obtain the maximum standardized uptake values (SUV_{max}), which were divided by blood pool uptake values in the right atrium (2 cm^2 area) to obtain TBR_{max} values. Given the difficulty in determining the exact borders of the mitral annulus, SUV_{mean}, and TBR_{mean} values were not quantified.

Uptake of ^{18}F-fluoride and ^{18}F-FDG in the aortic valve, aorta, and coronary arteries was measured as previously reported (Data Supplement).[15] BMD and ^{18}F-fluoride bone uptake were measured in 4 thoracic vertebrae as detailed previously.[18] Briefly, 0.5 cm^2 regions of interest were drawn within the cancellous bone. The average Hounsfield unit density within those regions was used as a relative measure of BMD.[22] Maximum ^{18}F-fluoride SUV values were quantified in the same regions of interest. Myocardial ^{18}F-FDG uptake was assessed by recording the maximum SUV in the left ventricular septum. A diffuse pattern of myocardial ^{18}F-FDG uptake accompanied by SUV ≥5.0 indicated failed myocardial suppression.[15] Patients with failed suppression were excluded from the analysis of FDG data, but not from analysis of ^{18}F-fluoride data.

Repeatability Studies

All CT and PET quantifications were independently performed in a blinded fashion by 2 trained observers (M.G. Trivieri and D. Massera). Disagreements were resolved by consensus with involvement of a third observer (R. Abgral).

Image Analysis: Echocardiography

Examination of the mitral valve apparatus was performed in a blinded fashion by one cardiologist (J. Andrews). At least 3 diastolic transmitral continuous-wave Doppler envelopes were traced to obtain an average diastolic transmitral gradient. Mitral regurgitation severity was assessed according to the American Society of Echocardiography guidelines.[23] No adjustment for heart rate was performed because 87% of patients had a heart rate of <80 bpm.

Disease Progression Studies

A subset of study participants underwent repeat CT and echocardiography using the same protocol and equipment 2 years after initial imaging. Mitral annular disease progression was assessed using the annualized change in CT calcium score and transmitral pressure gradient.

Statistical Analysis

Continuous variables are reported as mean±SD or median (interquartile range [IQR]) and were compared with the unpaired Student *t* test, Wilcoxon rank-sum or Kruskal-Wallis tests, as appropriate. Categorical variables are reported as proportions and analyzed with the χ^2 or Fishers exact test. Correlations were calculated using Spearman correlation coefficients. Data are presented by presence or absence of CT-MAC or mitral annular ^{18}F-fluoride activity or were dichotomized at the median CT-MAC calcium score. Bland-Altman mean differences and limits of agreement were obtained. Intraclass correlation coefficients were calculated with 2-way mixed-effects models. Multivariable linear and logistic regression models were used to identify predictors of MAC prevalence and ^{18}F-fluoride activity. Logarithmic transformation of ^{18}F-fluoride uptake was performed to achieve a normal distribution. Initially, all variables with $P<0.2$ in bivariate comparisons were included in the model, as well as important cardiovascular risk factors (age, sex, hypertension, diabetes mellitus, smoking, low-density lipoprotein cholesterol, and prior cardiovascular disease). Subsequently, a backward stepwise selection process was used with age and sex forced into the model. Separately, ^{18}F-FDG TBR_{max} was added to the model to identify FDG as a predictor of ^{18}F-fluoride uptake. Multiple linear and multinomial logistic regression models were used to identify predictors of MAC progression. All analyses were performed with STATA 14.2 (StataCorp LP, College Station, TX). A 2-tailed $P<0.05$ was used to define statistical significance.

RESULTS

Patient Population

The study cohort comprised 104 patients (mean age 72±8 years, 30% women; baseline characteristics are presented in Tables 1 and 2). The median transmitral mean diastolic pressure gradient was 1.4 (IQR, 1.0–2.1) mm Hg (Data Supplement). In addition, a control cohort of 17 subjects without heart valve calcification was included (68±8 years; Data Supplement). The effective radiation dose per patient was 9.7±1.2 mSv (CT conversion factor 0.014 mSv/mGy/cm). Interobserver reproducibility for MAC-CT calcium scoring (intraclass coefficient, 1.00 [95% CI, 0.99–1.00]) and PET quantifi-

Table 1. Baseline Characteristics by Presence of Mitral Annular Calcification (Prevalence) and Mitral Annular ^{18}F-Fluoride Uptake (Disease Activity)

Baseline Characteristics	MAC–, (n=69)	MAC+, (n=35)	*P* Value	^{18}F-Fluoride–, (n=66)	^{18}F-Fluoride+ (n=36)	*P* Value
Age, years	70.6±7.9	75.1±8.2	0.011	70.8±7.9	74.8±8.7	0.026
Female, n (%)	14 (20.3)	17 (48.6)	0.003	12 (18.2)	19 (52.8)	<0.001
Body mass index, kg/m^2	27.6±4.2	28.7±4.9	0.276	27.4±3.9	28.9±5.0	0.093
Ischemic heart disease, n (%)	27 (39.1)	11 (31.4)	0.441	28 (42.4)	9 (25.0)	0.080
Cardiovascular disease, n (%)	31 (44.9)	11 (31.4)	0.185	32 (48.9)	9 (25.0)	0.021
Current smoking, n (%)	8 (11.6)	4 (11.4)	0.980	7 (10.6)	4 (11.1)	0.937
Diabetes mellitus, n (%)	9 (13.2)	6 (17.1)	0.594	9 (13.9)	6 (16.7)	0.703
Hypertension, n (%)	41 (59.4)	23 (65.7)	0.533	39 (59.1)	23 (63.9)	0.635
Osteoporosis, n (%)	2 (2.9)	0 (0)	0.309	2 (3.0)	0 (0)	0.539
Bone mineral density (mean, HU)	160.6±43.2	142.1±38.5	0.035	159.7±41.0	144.8±43.6	0.096
eGFR, mL/min/1.73m^2	74.5±17.8	63.5±18.9	0.004	73.0±17.6	67.0±20.1	0.121
Urea, mg/dL	20.0±7.1	22.3±7.7	0.159	20.0±5.5	22.4±9.8	0.187
Calcium, mg/dL	9.3±0.7	9.4±0.3	0.119	9.2±0.5	9.5±0.7	0.047
Phosphate, mg/dL	3.6±1.1	3.5±0.5	0.606	3.5±0.5	3.7±1.4	0.411
Alkaline phosphatase, U/dL	78.7±20.2	99.1±74.9	0.133	80.2±22.9	95.6±74.3	0.255
Total cholesterol, mg/dL	195.6±52.6	183.8±51.5	0.280	190.2±50.1	193.2±56.2	0.781
LDL cholesterol, mg/dL	107.4±44.4	101.0±46.2	0.511	101.1±41.2	110.6±49.2	0.307
HDL cholesterol, mg/dL	55.4±23.2	50.4±12.0	0.146	55.8±23.4	50.5±12.4	0.133
Triglycerides, mg/dL	75.7±47.2	70.7±37.1	0.554	76.0±46.6	71.5±39.6	0.621
Lipoprotein(a), ng/dL	18.6 (8.9–62.9)	18.1 (9.0–54.9)	0.845	17.6 (8.3–67.4)	20.5 (9.0–55.6)	0.660
Statin therapy, n (%)	39 (56.5)	521 (60.0)	0.734	40 (60.6)	18 (50.0)	0.301
ACE inhibitor therapy, n (%)	27 (39.1)	14 (40.0)	0.932	26 (39.4)	14 (38.9)	0.960

Continuous variables are presented as mean±SD or median (IQR). eGFR indicates estimated glomerular filtration rate (CKD-EPI); HDL, high-density lipoprotein; LDL, low-density lipoprotein; and MAC, mitral annular calcification.

cation (^{18}F-fluoride TBR$_{max}$ 0.99 [0.98–0.99] and ^{18}F-FDG TBR$_{max}$ 0.87 [0.82–0.91]) was good (Data Supplement).

Factors Associated with MAC Prevalence

The median baseline MAC-CT calcium score was 0 (IQR, 0–316) AU and was higher in women (283 [0–1082] AU) compared with men (0 [0–0] AU; *P*=0.001). Overall, 35 (33.7%) patients had MAC on CT (CT+; 837 [300–2129] AU), who were older, twice as likely to be female, had more AVC, lower BMD, and reduced estimated glomerular filtration rate (eGFR) compared with patients without MAC (CT–). Both groups had extensive cardiovascular disease risk factor burden (Table 1). In a multiple logistic regression model, female sex and AVC calcium score were statistically significantly associated with MAC prevalence (Table 3).

Mitral Annular Inflammatory Activity (^{18}F-FDG PET)

Thirty-three patients (32%) met criteria for failed myocardial suppression of physiological ^{18}F-FDG uptake and were excluded from further analysis of FDG data only. In the remaining patients, median mitral annular ^{18}F-FDG TBR$_{max}$ was 1.21 (IQR, 1.14–1.39), higher in patients with CT-MAC (CT+ 1.44 [1.37–1.58]) compared with those without (CT– 1.17 [1.12–1.24]; *P*<0.001) or with controls (1.06 [1.04–1.17]; *P*<0.001). A moderate correlation was observed between mitral annular ^{18}F-FDG TBR$_{max}$ and CT-MAC scores (*r*=0.50, *P*<0.001; Table 4).

Mitral annular ^{18}F-FDG TBR$_{max}$ uptake was negatively correlated with total cholesterol and low-density lipoprotein (*r*=–0.30; *P*=0.014) and was higher in women (1.33 [1.16–1.45]) than men (1.19 [1.12–1.32]; *P*=0.037); there was no correlation with other serum biomarkers nor ^{18}F-FDG activity measured in remote areas (aortic valve, *r*=–0.05, *P*=0.658; aorta, *r*=–0.23, *P*=0.060; Table 4).

MAC Activity (^{18}F-Fluoride PET)

Median mitral annular ^{18}F-fluoride TBR$_{max}$ uptake in the entire study cohort (104 patients) was 1.44 (IQR, 1.27–1.89). Patients with CT-MAC had higher ^{18}F-fluoride uptake (CT+ 2.32 [1.81–3.27]) than those without (CT– 1.30 [1.22–1.49]; *P*<0.001). Mitral annular ^{18}F-fluoride activity appeared most closely related to local markers of disease burden. A strong correlation was observed

Table 2. Imaging Characteristics by Presence of Mitral Annular Calcification (Prevalence) and Mitral Annular ^{18}F-Fluoride Uptake (Disease Activity)

Imaging Characteristics	MAC–, (n=69)	MAC+, (n=35)	*P* Value	^{18}F-Fluoride–, (n=66)	^{18}F-Fluoride+, (n=36)	*P* Value
Aortic valve by echocardiography						
Control, n (%)	3 (4.4)	2 (5.7)	0.034	4 (6.1)	1 (2.8)	0.012
Sclerosis, n (%)	16 (23.3)	2 (5.7)		17 (25.8)	1 (2.8)	
Mild stenosis, n (%)	20 (29.0)	5 (14.3)		17 (25.8)	7 (19.4)	
Moderate stenosis, n (%)	18 (26.1)	15 (42.9)		18 (27.3)	15 (41.7)	
Severe stenosis, n (%)	12 (17.4)	11 (31.4)		10 (15.2)	12 (33.3)	
AVC calcium score, AU	801 (298–2174)	1501 (600–3314)	0.030	771 (309–2076)	1598 (1007–3230)	0.003
MAC calcium score, AU	0	837 (300–2129)	…	0	834 (139–2107)	…
Aorta calcium score, AU	894 (190–2548)	1733 (396–7984)	0.058	997 (144–3181)	1378 (374–4036)	0.170
Aortic valve ^{18}F-fluoride TBR_{max}	2.44 (1.91–2.99)	2.58 (2.21–3.14)	0.192	2.34 (1.96–2.91)	2.74 (2.38–3.18)	0.028
Mitral annulus ^{18}F-fluoride TBR_{max}	1.30 (1.22–1.49)	2.32 (1.81–3.27)	<0.001	1.29 (1.22–1.41)	2.30 (1.84–3.07)	<0.001
Coronary artery^{18}F fluoride TBR_{max}	1.50 (1.33–1.75)	1.60 (1.35–2.09)	0.274	1.50 (1.35–1.76)	1.59 (1.35–2.02)	0.590
^{18}F-fluoride TBR_{max} in aorta	2.06 (1.82–2.28)	2.14 (1.19–2.38)	0.081	2.05 (1.84–2.26)	2.20 (1.91–2.50)	0.060
Aortic valve ^{18}F-FDG TBR_{max} *	1.52 (1.44–1.63)	1.39 (1.33–1.63)	0.072	1.51 (1.40–1.63)	1.46 (1.35–1.68)	0.83
Mitral annulus ^{18}F-FDG TBR_{max} *	1.17 (1.12–1.24)	1.44 (1.37–1.58)	<0.001	1.17 (1.12–1.26)	1.38 (1.24–1.56)	0.002
Aorta ^{18}F-FDG TBR_{max}	1.84 (1.69–1.94)	1.68 (1.50–1.78)	0.002	1.83 (1.68–1.92)	1.69 (1.61–1.83)	0.116

Continuous variables are presented as median (IQR). AVC indicates aortic valve calcification; ^{18}F-FDG, ^{18}F-Fluorodeoxyglucose; MAC, mitral annular calcification; and TBR_{max}, tissue-to-background ratio.

* n=33 patient with failed myocardial FDG suppression were excluded.

between mitral annular ^{18}F-fluoride activity and baseline CT-MAC score (r=0.79, P<0.001; Figure 1A) while a moderate correlation was observed with ^{18}F-FDG uptake (r=0.32, P=0.001; Figure 1B). By comparison, modest or no correlations were observed between mitral annular ^{18}F-fluoride uptake and uptake in other areas (aorta, r=0.23, P=0.025; aortic valve, r=0.19, P=0.053; coronary arteries, r=0.14, P=0.159; and bone, r=0.02, P=0.861) or serum biomarkers including calcium, alkaline phosphatase, and lipid markers (Table 3). Mitral annular ^{18}F-fluoride uptake was higher in women compared with men (2.01 [1.31–2.69] versus 1.36 [1.26–1.63]; P=0.002), and in patients with impaired (eGFR<60 mL/min/1.73m^2) compared with preserved renal function (1.39 [1.10–1.61] versus 1.26 [1.04–1.36]; P=0.046).

Among the control cohort, the highest ^{18}F-fluoride TBR_{max} value was 1.64. This cutoff was used to categorize patients in the study cohort as having increased ^{18}F-fluoride uptake (>1.64, PET+) or not (≤1.64, PET–). Overall, 36 (35.6%) patients had increased ^{18}F-fluoride uptake (median TBR_{max}, 2.30 [1.84–3.07]). PET+ patients had a median CT-MAC calcium score of 834 (139–2107), while PET– patients had no MAC (Figure 1C). Compared with PET– patients, PET+ patients were older, more likely to be female, had more AVC, lower BMD, and eGFR (Table 1). In a multiple linear regression model, CT-MAC and AVC calcium scores, female sex, and eGFR demonstrated a statistically significant association with MAC disease activity. When ^{18}F-FDG TBR_{max} was added to the model, significant predictors of MAC ^{18}F-fluoride activity were baseline CT-MAC and ^{18}F-FDG TBR_{max} in the subset of patients with successful myocardial suppression (Table 5).

Table 3. Factors Associated With MAC Prevalence in a Multiple Logistic Regression Model

	OR	95% CI	*P* Value
Age (per 10 y)	1.29	0.67–2.50	0.45
Male sex	0.25	0.11–0.75	0.01
Aortic valve calcium (per 100 AU increase)	1.03	1.00–1.06	0.03
eGFR (per 10 mL/min)	0.77	0.59–1.01	0.06

eGFR indicates estimated glomerular filtration rate; MAC, mitral annular calcification; and OR, odds ratio.

Disease Progression in Mitral Annular Calcification

Sixty patients in the study cohort underwent repeat echocardiography and CT after a median of 741 (IQR, 726–751) days (Figure 2 includes examples of 3 patients). The annual progression rate of CT-MAC calcium score was 2 (0–166) AU per year. The strongest associations of MAC progression were observed with baseline CT-MAC (r=0.82, P<0.001; Figure 3A), ^{18}F-fluoride (r=0.75, P<0.001; Figure 3B) and ^{18}F-FDG activity (r=0.48; P<0.002). Women tended to have a higher rate of MAC progression (34 [0–409] AU/y) than men (0 [0–68] AU/y; P=0.083). There was no association between baseline eGFR and MAC progression (r=–0.13; P=0.308) nor differences in the rate of MAC progression between those with and without advanced

Table 4. Correlations of Mitral Annular ^{18}F-Fluoride and ^{18}F-FDG PET Uptake (Disease Activity) With Imaging Findings in the Mitral Annulus (Local Factors) and Remote Regions, as Well as Serum Biomarker Levels (Remote Factors)

	^{18}F-Fluoride TBR_{max}		^{18}F-FDG TBR_{max}	
	r Value	*P* Value	*r* Value	*P* Value
Local factors				
Mitral annulus CT calcium score	0.78	<0.001	0.50	<0.001
Mitral annulus ^{18}F-fluoride TBR_{max}	…	…	0.54	<0.001
Mitral annulus ^{18}F-FDG TBR_{max}	0.54	<0.001	…	…
Remote factors				
Aortic valve CT calcium score	0.24	0.017	0.15	0.218
Aortic valve ^{18}F-fluoride TBR_{max}	0.19	0.053	–0.02	0.848
Aortic valve ^{18}F-FDG TBR_{max}	–0.02	0.895	–0.05	0.658
Coronary artery CT calcium score	0.03	0.789	0.12	0.327
Coronary artery ^{18}F-fluoride TBR_{max}	0.14	0.159	0.08	0.518
Aorta CT calcium score	0.20	0.049	0.14	0.262
Aorta ^{18}F-fluoride TBR_{max}	0.23	0.025	–0.02	0.884
Aorta ^{18}F-FDG TBR_{max}	–0.16	0.127	–0.23	0.060
Bone mineral density	–0.19	0.065	–0.15	0.247
Bone ^{18}F-fluoride TBR_{max}	0.02	0.861	0.01	0.989
Serum biomarkers				
Calcium	0.15	0.126	0.04	0.774
Phosphate	–0.02	0.828	0.14	0.260
Alkaline phosphatase	0.11	0.264	–0.02	0.887
Creatinine	0.07	0.494	–0.02	0.848
LDL cholesterol	–0.03	0.746	–0.30	0.014
HDL cholesterol	–0.04	0.677	–0.01	0.919
Total cholesterol	–0.07	0.500	–0.24	0.050
Triglycerides	–0.07	0.484	0.00	0.992
Lipoprotein(a)	0.11	0.286	0.08	0.507

Data presented in study cohort patients (n=104). In ^{18}F-FDG analyses, patients with failed myocardial suppression were excluded (n=33). CT indicates computed tomography; ^{18}F-FDG, ^{18}F-Fluorodeoxyglucose; HDL, high-density lipoprotein; LDL, low-density lipoprotein; PET, positron emission tomography; and TBR_{max}, tissue-to-background ratio.

chronic kidney disease (*P*=0.933). There were no associations with MAC progression for low-density lipoprotein (*r*=–0.10; *P*=0.444), HDL (high-density lipoprotein; *r*=–0.08, *P*=0.524) or lipoprotein(a) (*r*=0.07, *P*=0.629).

All 22 (36.7%) patients with baseline CT-MAC (CT+) demonstrated progression in their CT-MAC scores (median progression rate 199 [63–480] AU/y). Eight (21.1%) of the 38 patients without baseline CT-MAC (CT–) developed new MAC (CT-MAC score at second exam 135 [40–291] AU). MAC regression was not observed. In a multiple linear regression model, baseline CT-MAC calcium score (β=0.048 per 100 AU; *P*=0.013) was an independent predictor of log-transformed MAC progression after adjustment for age (β=0.008 per year; *P*=0.847), sex (β=–0.580; *P*=0.368) and eGFR (β=–0.063 per 10 mL/min; *P*=0.718).

Patients with increased mitral annular ^{18}F-fluoride PET uptake demonstrated faster progression than patients without (CT-MAC progression: PET+ 200 [47–480] versus PET– 0 [0–3] AU/y; *P*<0.001). In multinomial logistic regression models adjusted for age and sex, there was a stronger association of positive ^{18}F-fluoride PET uptake (PET+) with a MAC progression rate above median (OR, 100.03; 95% CI 10.88–919.62; *P*<0.001), than below median (OR, 17.25; 95% CI 2.76–107.92; *P*=0.002). Similar results were obtained with ^{18}F-fluoride uptake as continuous variable (MAC progression above median: OR, 1.95 per 0.1 increment in TBR_{max}; 95% CI 1.38–2.75, *P*<0.001; MAC progression below median: OR, 1.71; 95% CI 1.23–2.37; *P*=0.001).

When considering PET and CT data together, PET–CT– patients did not demonstrate MAC progression (median MAC progression, 0 [0–0] AU/y, n=32), while MAC progression was highest in PET+CT+ patients (270 [68–493] AU/y, n=18). Intermediate progression was observed in PET+CT– (47 [0–95] AU/y, n=5) and PET–CT+ patients (102 [39–166] AU/y, n=4; Figure 3C).

DISCUSSION

We used state-of-the-art multimodality imaging to investigate MAC, providing novel insights into the pathophysiology of this common condition and factors associated with its prevalence, disease activity, and progression. We confirmed that MAC is characterized by both calcification and inflammatory activity that increases proportionally to the baseline MAC burden. Importantly, while female sex, renal dysfunction, and local inflammatory activity were associated with MAC disease activity, the strongest correlate was the local burden of calcium already present within the valve annulus. Similar observations were made with respect to progression, with the fastest progression observed in patients with the largest baseline burden of MAC. We, therefore, suggest that once established, MAC activity and progression are characterized by a vicious cycle of established calcium, injury, and inflammation within the valve that prompts further calcification activity. These findings support the concept that therapeutic strategies targeting MAC will need focus on breaking this vicious calcification cycle.

Despite its high prevalence, contribution to mitral valve dysfunction and adverse prognosis,[4] the pathobiology of MAC remains incompletely understood. Moreover, therapeutic options are limited since effective medical therapy is lacking and surgical intervention is made complicated by its presence.[24] There is, there-

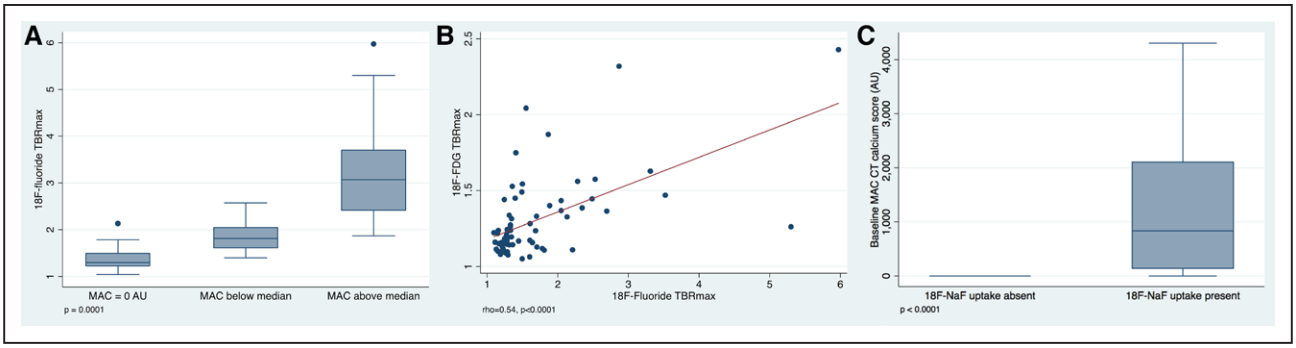

Figure 1. Relationship of mitral annular calcification (MAC) ^{18}F-fluoride activity, MAC calcium score, and ^{18}F-FDG activity.
MAC activity (^{18}F-fluoride tissue-to-background ratio [TBRmax]) increased with the burden of baseline MAC (box plots by categories of baseline CT-MAC calcium score: zero/below median [<837 AU]/above median [≥837 AU]; **A**) and was correlated with inflammatory activity $_{18}$F-fluorodeoxyglucose ($_{18}$F-FDG TBRmax; **B**). Baseline CT-MAC was virtually absent in patients without ^{18}F-fluoride activity (**C**). CT indicates computed tomography.

fore, an urgent need to illuminate the pathophysiology underlying MAC and to identify novel therapeutic strategies to prevent its clinical sequelae.[9] We describe a new multimodality imaging approach to help address this need. First, we have applied CT calcium scoring to define the presence of MAC and to quantify disease prevalence, burden, and progression. Second, we used ^{18}F-FDG to measure inflammatory activity. Although ^{18}F-FDG was only interpretable in two-thirds of patients, our data clearly demonstrate that MAC is an inflammatory condition with the ^{18}F-FDG PET signal increasing in proportion to baseline disease severity. Finally, we used ^{18}F-fluoride PET as marker of calcification activity demonstrating a close association with subsequent progression and building upon a growing body of literature using ^{18}F-fluoride to image developing cardiovascular microcalcification. The use of a cohort of patients with calcific aortic valve disease provided a patient population at high risk of developing MAC, as evidenced by the particularly high prevalence. This gave us the opportunity to assess disease activity and progression in patients with established MAC, but also in patients who subsequently developed MAC during follow-up. It also provided insights into why certain patients with aortic stenosis develop MAC, while others do not, with female sex, renal impairment, and advanced AVC appearing to be of particular importance in this population.

Factors Associated With Disease Activity in MAC

Using ^{18}F-fluoride PET, we demonstrated that calcification activity in the mitral annulus is closely related to the local inflammatory signal provided by ^{18}F-FDG imaging. This is consistent with histological studies of excised mitral valves demonstrating increased expression of pro-calcific cells and mediators adjacent to T-lymphocytic infiltrates and suggests that calcium deposition is closely related to inflammatory activity.[5,6] However, MAC activity was, in fact, most closely associated with the baseline CT-MAC calcium score. Similar results were observed for progression: patients with rapid disease progression and highest disease activity were those with the highest baseline CT calcium scores. Indeed, baseline MAC was the strongest predictor of MAC progression, here replicating the findings from the Multiethnic Study of Atherosclerosis.[7]

We believe our concordant data on MAC disease activity and progression have important therapeutic implications. The findings are remarkably similar to observations made in aortic stenosis, where it has been suggested that calcium within the valve increases mechanical stress and injury leading to inflammation and increased calcification activity.[25] A similar self-perpetuating cycle of calcification inducing further calcification

Table 5. Factors Associated With Disease Activity in MAC

	Model 1 (n=98)			Model 2 (n=68)		
	β Value	95% CI	*P* Value	β Value	95% CI	*P* Value
Age (per 10 y)	−0.002	−0.070 to 0.066	0.953	0.065	−0.019 to 0.148	0.127
Male sex	−0.172	−0.289 to −0.054	0.005	−0.082	−0.229 to 0.066	0.273
AVC (per 100 AU)	0.003	−0.000 to 0.005	0.052	0.002	−0.002 to 0.005	0.318
eGFR (per 10 mL/min)	−0.032	−0.061 to −0.003	0.030	−0.001	−0.039 to 0.038	0.988
MAC (per 100 AU)	0.014	0.011 to 0.018	<0.001	0.010	0.005 to 0.015	<0.001
^{18}F-FDG TBR_{max} (per 0.1)	…	…	…	0.049	0.021 to 0.077	0.001

Predictors of log-transformed ^{18}F-fluoride TBR_{max} in multiple linear regression model. Model 1 includes age, sex, hypertension, diabetes mellitus, smoking, LDL, prior cardiovascular disease, and variables with *P*>0.2 in bivariate comparisons, followed by backwards stepwise elimination process. Model 2 includes ^{18}F-FDG TBR_{max} in addition to variables in model 1. AVC indicates aortic valve calcification; ^{18}F-FDG, ^{18}F-Fluorodeoxyglucose; MAC, mitral annular calcification; and TBR_{max}, tissue-to-background ratio.

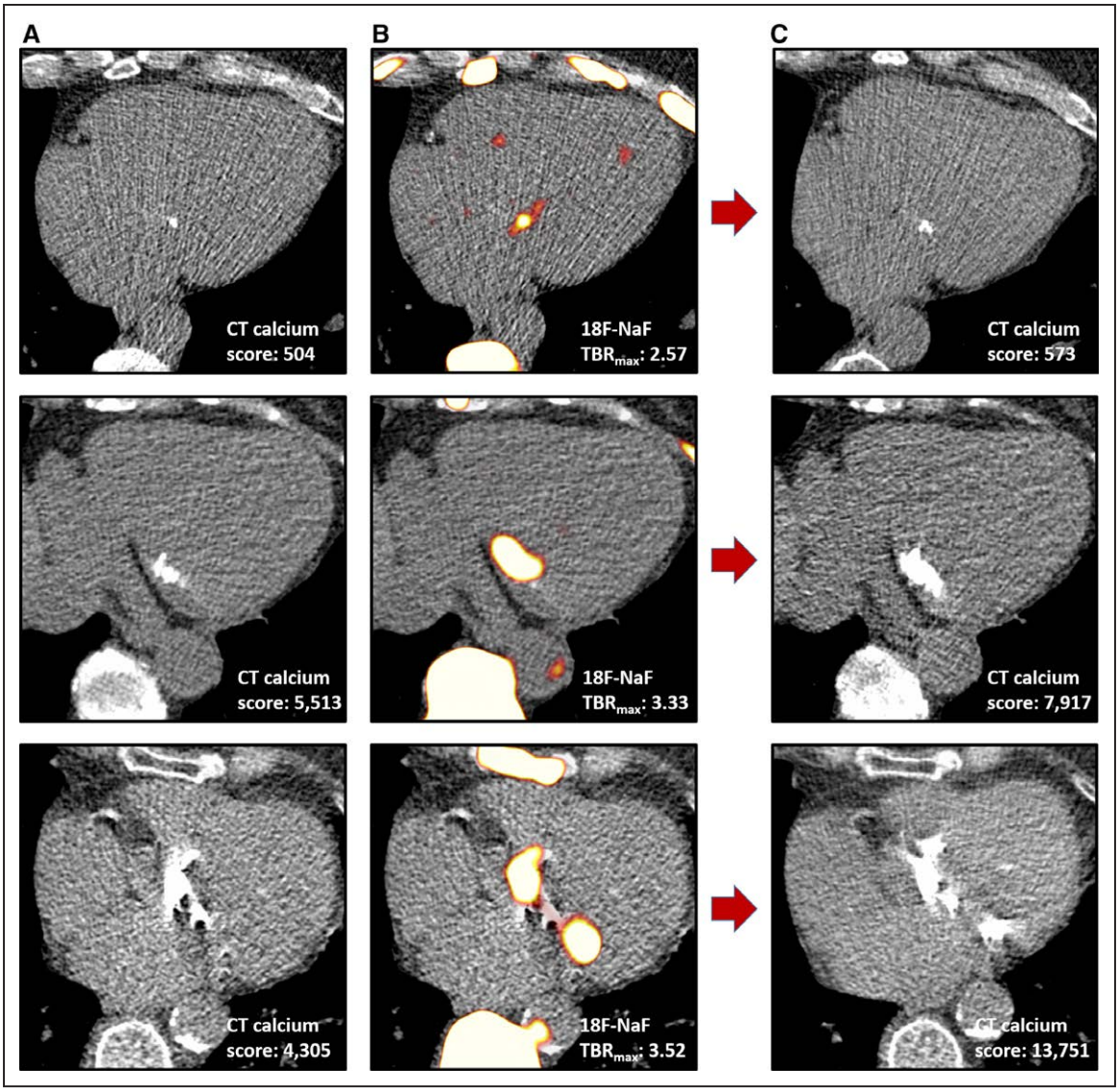

Figure 2. Baseline computed tomography mitral annular calcification (CT-MAC), ^{18}F-fluoride positron emission tomography (PET) activity, and 2-year progression in 3 patients.
First row, Mild MAC at baseline (**A**), associated with mild mitral annular ^{18}F-fluoride uptake (**B**) and modest progression after 2 y (change in CT-MAC 69 AU (**C**). **Second row**, Moderate MAC at baseline (**A**), moderate ^{18}F-fluoride uptake (**B**), and intermediate progression after 2 y (change in CT-MAC 2404 AU (**C**). **Third row**, Severe MAC at baseline (**A**), bifocal high-intensity ^{18}F-fluoride uptake (**B**), and rapid progression (change in CT-MAC 9446 AU (**C**). Note de novo areas of MAC that developed at the site of intense ^{18}F-fluoride uptake in the lateral annulus.

might also underlie MAC. The development of effective medical therapy in both conditions is, therefore, likely to require strategies that interrupt this cycle without impacting bone health. Studies are currently underway testing such therapies in patients with aortic stenosis (SALTIRE2, NCT02132026) providing an opportunity to investigate their impact on bystander MAC.

Study Limitations

Our study cohort comprised participants with calcific aortic valve disease. Although this ensured high proportions of prevalent and incident MAC, our results may not directly apply to patients with isolated mitral valve disease or other conditions known to be associated with MAC. Moreover, our sample size was modest, precluding more detailed examination of determinants and consequences of microcalcification and inflammation. In addition, one-third of patients met criteria for failed myocardial FDG suppression and were excluded from the analysis of FDG data. Further studies exploring the role of PET-CT in larger samples and different patient populations are warranted. Such studies may benefit from the use of contrast CT to better investigate the spatial distribution of PET uptake within the mitral annulus and to improve interobserver reproducibility. In addition, advanced imaging processing technologies such as adaptive thresholding may improve uptake delineation, and ECG-gating of the PET acquisition may reduce image blurring because of cardiac motion.

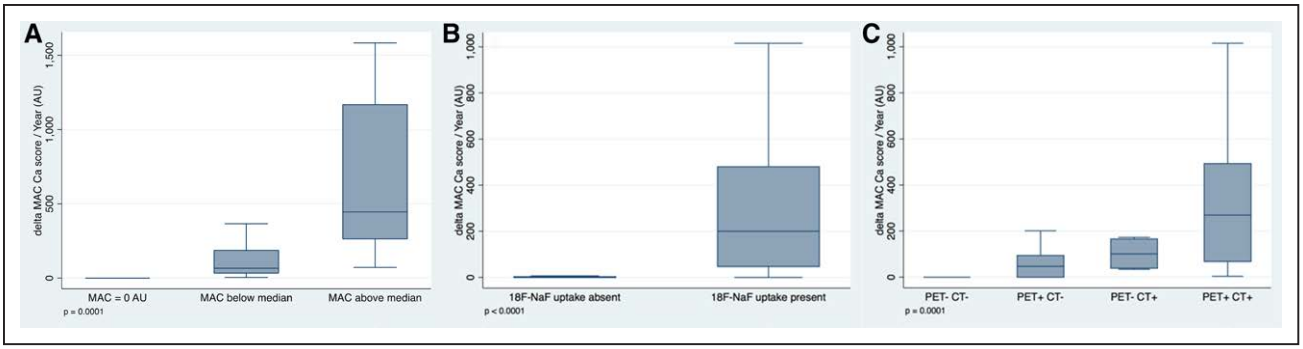

Figure 3. Relationship of mitral annular calcification (MAC) progression with baseline MAC calcium score and ^{18}F-fluoride activity.
MAC progression (AU/y) increased with the burden of baseline MAC (box plots by categories of baseline CT-MAC calcium score: zero/below median [<837 AU]/above median [≥837 AU]) (**A**) and was virtually absent in patients without ^{18}F-fluoride activity (**B**). A steady increase in MAC progression was observed on moving from ^{18}F-fluoride PET−CT− to PET−CT+, to PET+CT−, and finally to PET+CT+ patients (**C**). CT indicates computed tomography; and PET, positron emission tomography.

Conclusions

In this cohort, although female sex, renal dysfunction, and local inflammatory activity emerged as important determinants of disease activity in MAC, the strongest determinant was the baseline CT-MAC calcium score. Moreover, the higher the baseline burden of MAC, the higher the disease activity and the faster the rate of progression. This may reflect a vicious cycle of established calcium begetting further calcification within the mitral annulus that may be a suitable target of future therapies.

ARTICLE INFORMATION

Received June 29, 2018; accepted January 2, 2019.

The Data Supplement is available at https://www.ahajournals.org/doi/suppl/10.1161/CIRCIMAGING.118.008513.

Correspondence

Marc R. Dweck, MD, PhD, British Heart Foundation Centre for Cardiovascular Sciences, University of Edinburgh, 49 Little France Crescent, Edinburgh, EH164SB, United Kingdom. Email marc.dweck@ed.ac.uk

Affiliations

Leon H. Charney Division of Cardiology, New York University School of Medicine, New York, NY (D.M.); Department of Cardiology, Icahn School of Medicine at Mount Sinai, New York, NY (M.G.T., S.S.); British Heart Foundation Centre for Cardiovascular Science, University of Edinburgh, United Kingdom (J.P.M.A., A.R.C., W.S.A.J., A.T.V., M.K.D., T.A.P., D.E.N., M.R.D.); Department of Nuclear Medicine, University Hospital of Brest, France (R.A.); Department of Vascular Medicine, Academic Medical Center, Amsterdam, The Netherlands (K.H.Z.); and Cardiology Section, San Francisco Veterans Affairs Health Care System and Department of Epidemiology and Biostatistics, University of California, San Francisco, CA (J.R.K.).

Sources of Funding

D. Massera was supported by The Glorney-Raisbeck Fellowship Program, Corlette Glorney Foundation and The New York Academy of Medicine; M.G. Trivieri was supported by the KL2 TR001435 from the Institute for Translational Science, Icahn School of Medicine, Mount Sinai; J.P.M. Andrews and A.R. Chapman were supported by British Heart Foundation (BHF) Clinical Research Training Fellowship No. FS/17/51/33096 and FS/16/75/32533; J.R. Kizer was supported by K24 Hl135413 from the National Heart, Lung, and Blood Institute; D.E. Newby was supported by the BHF (CH/09/002, RE/13/3/30183, and RM/13/2/30158) and has received a Wellcome Trust Senior Investigator Award (WT103782AIA); and M.R. Dweck was supported by the BHF (FS/14/78/31020) and is the recipient of the Sir Jules Thorn Award for Biomedical Research 2015.

Disclosures

J.R. Kizer reports stock ownership in Amgen, Gilead Sciences, Johnson & Johnson, and Pfizer. The other authors report no conflicts.

REFERENCES

1. Allison MA, Cheung P, Criqui MH, Langer RD, Wright CM. Mitral and aortic annular calcification are highly associated with systemic calcified atherosclerosis. *Circulation*. 2006;113:861–866. doi: 10.1161/CIRCULATIONAHA.105.552844
2. Barasch E, Gottdiener JS, Larsen EK, Chaves PH, Newman AB, Manolio TA. Clinical significance of calcification of the fibrous skeleton of the heart and aortosclerosis in community dwelling elderly. The Cardiovascular Health Study (CHS). *Am Heart J*. 2006;151:39–47. doi: 10.1016/j.ahj.2005.03.052
3. Kizer JR, Wiebers DO, Whisnant JP, Galloway JM, Welty TK, Lee ET, Best LG, Resnick HE, Roman MJ, Devereux RB. Mitral annular calcification, aortic valve sclerosis, and incident stroke in adults free of clinical cardiovascular disease: the Strong Heart Study. *Stroke*. 2005;36:2533–2537. doi: 10.1161/01.STR.0000190005.09442.ad
4. Fox CS, Vasan RS, Parise H, Levy D, O'Donnell CJ, D'Agostino RB, Benjamin EJ; Framingham Heart Study. Mitral annular calcification predicts cardiovascular morbidity and mortality: the Framingham Heart Study. *Circulation*. 2003;107:1492–1496.
5. Mohler ER 3rd, Gannon F, Reynolds C, Zimmerman R, Keane MG, Kaplan FS. Bone formation and inflammation in cardiac valves. *Circulation*. 2001;103:1522–1528.
6. Arounlangsy P, Sawabe M, Izumiyama N, Koike M. Histopathogenesis of early-stage mitral annular calcification. *J Med Dent Sci*. 2004;51:35–44.
7. Elmariah S, Budoff MJ, Delaney JA, Hamirani Y, Eng J, Fuster V, Kronmal RA, Halperin JL, O'Brien KD. Risk factors associated with the incidence and progression of mitral annulus calcification: the multi-ethnic study of atherosclerosis. *Am Heart J*. 2013;166:904–912. doi: 10.1016/j.ahj.2013.08.015
8. Labovitz AJ, Nelson JG, Windhorst DM, Kennedy HL, Williams GA. Frequency of mitral valve dysfunction from mitral anular calcium as detected by Doppler echocardiography. *Am J Cardiol*. 1985;55:133–137.
9. Sud K, Agarwal S, Parashar A, Raza MQ, Patel K, Min D, Rodriguez LL, Krishnaswamy A, Mick SL, Gillinov AM, Tuzcu EM, Kapadia SR. Degenerative mitral stenosis: unmet need for percutaneous interventions. *Circulation*. 2016;133:1594–1604. doi: 10.1161/CIRCULATIONAHA.115.020185
10. Kanjanauthai S, Nasir K, Katz R, Rivera JJ, Takasu J, Blumenthal RS, Eng J, Budoff MJ. Relationships of mitral annular calcification to cardiovascular risk factors: the Multi-Ethnic Study of Atherosclerosis (MESA). *Atherosclerosis*. 2010;213:558–562. doi: 10.1016/j.atherosclerosis.2010.08.072
11. Linefsky JP, O'Brien KD, Katz R, de Boer IH, Barasch E, Jenny NS, Siscovick DS, Kestenbaum B. Association of serum phosphate levels with aortic valve sclerosis and annular calcification: the cardiovascular health study. *J Am Coll Cardiol*. 2011;58:291–297. doi: 10.1016/j.jacc.2010.11.073
12. Asselbergs FW, Mozaffarian D, Katz R, Kestenbaum B, Fried LF, Gottdiener JS, Shlipak MG, Siscovick DS. Association of renal function with cardiac calcifications in older adults: the cardiovascular health study. *Nephrol Dial Transplant*. 2009;24:834–840. doi: 10.1093/ndt/gfn544

13. Bortnick AE, Bartz TM, Ix JH, Chonchol M, Reiner A, Cushman M, Owens D, Barasch E, Siscovick DS, Gottdiener JS, Kizer JR. Association of inflammatory, lipid and mineral markers with cardiac calcification in older adults. *Heart*. 2016;102:1826–1834. doi: 10.1136/heartjnl-2016-309404
14. Massera D, Xu S, Bartz TM, Bortnick AE, Ix JH, Chonchol M, Owens DS, Barasch E, Gardin JM, Gottdiener JS, Robbins JR, Siscovick DS, Kizer JR. Relationship of bone mineral density with valvular and annular calcification in community-dwelling older people: the Cardiovascular Health Study. *Arch Osteoporos*. 2017;12:52. doi: 10.1007/s11657-017-0347-y
15. Dweck MR, Jones C, Joshi NV, Fletcher AM, Richardson H, White A, Marsden M, Pessotto R, Clark JC, Wallace WA, Salter DM, McKillop G, van Beek EJ, Boon NA, Rudd JH, Newby DE. Assessment of valvular calcification and inflammation by positron emission tomography in patients with aortic stenosis. *Circulation*. 2012;125:76–86. doi: 10.1161/CIRCULATIONAHA.111.051052
16. Irkle A, Vesey AT, Lewis DY, Skepper JN, Bird JL, Dweck MR, Joshi FR, Gallagher FA, Warburton EA, Bennett MR, Brindle KM, Newby DE, Rudd JH, Davenport AP. Identifying active vascular microcalcification by (18)F-sodium fluoride positron emission tomography. *Nat Commun*. 2015;6:7495. doi: 10.1038/ncomms8495
17. Blau M, Ganatra R, Bender MA. 18 F-fluoride for bone imaging. *Semin Nucl Med*. 1972;2:31–37.
18. Dweck MR, Khaw HJ, Sng GK, Luo EL, Baird A, Williams MC, Makiello P, Mirsadraee S, Joshi NV, van Beek EJ, Boon NA, Rudd JH, Newby DE. Aortic stenosis, atherosclerosis, and skeletal bone: is there a common link with calcification and inflammation? *Eur Heart J*. 2013;34:1567–1574. doi: 10.1093/eurheartj/eht034
19. Rudd JH, Warburton EA, Fryer TD, Jones HA, Clark JC, Antoun N, Johnström P, Davenport AP, Kirkpatrick PJ, Arch BN, Pickard JD, Weissberg PL. Imaging atherosclerotic plaque inflammation with [18F]-fluorodeoxyglucose positron emission tomography. *Circulation*. 2002;105:2708–2711.
20. Tsimikas S, Lau HK, Han KR, Shortal B, Miller ER, Segev A, Curtiss LK, Witztum JL, Strauss BH. Percutaneous coronary intervention results in acute increases in oxidized phospholipids and lipoprotein(a): short-term and long-term immunologic responses to oxidized low-density lipoprotein. *Circulation*. 2004;109:3164–3170. doi: 10.1161/01.CIR.0000130844.01174.55
21. Agatston AS, Janowitz WR, Hildner FJ, Zusmer NR, Viamonte M Jr, Detrano R. Quantification of coronary artery calcium using ultrafast computed tomography. *J Am Coll Cardiol*. 1990;15:827–832.
22. Romme EA, Murchison JT, Phang KF, Jansen FH, Rutten EP, Wouters EF, Smeenk FW, Van Beek EJ, Macnee W. Bone attenuation on routine chest CT correlates with bone mineral density on DXA in patients with COPD. *J Bone Miner Res*. 2012;27:2338–2343. doi: 10.1002/jbmr.1678
23. Zoghbi WA, Adams D, Bonow RO, Enriquez-Sarano M, Foster E, Grayburn PA, Hahn RT, Han Y, Hung J, Lang RM, Little SH, Shah DJ, Shernan S, Thavendiranathan P, Thomas JD, Weissman NJ. Recommendations for noninvasive evaluation of native valvular regurgitation: a report from the American Society of Echocardiography developed in collaboration with the Society for Cardiovascular Magnetic Resonance. *J Am Soc Echocardiogr*. 2017;30:303–371. doi: 10.1016/j.echo.2017.01.007
24. Carpentier AF, Pellerin M, Fuzellier JF, Relland JY. Extensive calcification of the mitral valve anulus: pathology and surgical management. *J Thorac Cardiovasc Surg*. 1996;111:718–729; discussion 729–730.
25. Pawade TA, Newby DE, Dweck MR. Calcification in aortic stenosis: the skeleton key. *J Am Coll Cardiol*. 2015;66:561–577. doi: 10.1016/j.jacc.2015.05.066